

A Modal Solution for Wave Propagation in Finite Shells of Revolution

J. P. RANEY* AND J. T. HOWLETT†
NASA Langley Research Center, Hampton, Va.

This analysis presents a comparison of the modal superposition method of solution for wave propagation with the method of characteristics and finite differences. Solutions for displacements and stress resultants for axisymmetric wave propagation due to initial velocity conditions and for time-varying edge conditions are obtained. The modal equations are constructed using modes generated by a new finite-element shell program. Closed-form solution of the modal equations is employed so that time-consuming numerical integration is not required. The participation of each mode is computed so that modes which contribute heavily to the solution can be individually examined for accuracy. Comparisons are given which support the conclusions that the modal approach is accurate and efficient and provides insights not offered by the other methods. The paper concludes with the solution, for displacement response, of a ring-stiffened shell to separate axial and a radial initial velocity conditions.

Nomenclature

C_p	= $[E/\rho(1 - \nu^2)]^{1/2}$ = plate velocity
C_s	= $k(G/\rho)^{1/2}$ = shear velocity
E	= elastic modulus
F_2	= $1 - \eta/R$
$\{f(t)\}$	= generalized force vector
g	= $k^2(1 - \nu)/2$
h	= shell thickness
$[K], [\bar{K}], [K]$	= shell stiffness matrices
k^2	= shear correction factor
L	= shell length
$[M], [\bar{M}], [M]$	= shell mass matrices
$\{\bar{q}\}, \{q\}$	= normal coordinate vectors
R	= shell radius
u	= axial displacement
v	= tangential displacement
w	= radial displacement
$\{y\}, \{\bar{y}\}, \{y\}$	= physical coordinate vectors
η	= $h^2/12 R$
γ, ρ	= unit weight, unit mass
λ_i	= i th eigenvalue
ν	= Poisson's ratio
$[\bar{\phi}], [\phi]$	= modal matrices
ψ	= rotation about reference surface

Introduction

THE theory of elastic wave propagation in solids was developed by Love, Stokes, Poisson, Rayleigh, Kelvin, and others and is concisely reviewed and summarized by Kolsky.¹ A recent symposium on "Wave Propagation in Solids" sponsored by the ASME² includes, in a primarily theoretical approach emphasizing the transform approach and closed-form solutions, treatment of wave propagation in bounded elastic media. Well-developed theory and approximate closed-form solutions to basic problems are useful in providing physical in-

sight into the fundamental phenomena of wave propagation. However, closed-form solutions such as those obtained by application of transform methods are not feasible for many structures of engineering importance such as finite, ring-stiffened, shells of revolution. Analytical approaches which concentrate on efficient numerical solution are needed to cope with wave propagation problems associated with high energy impact and explosive shock in shell structures.

The advent of the high-speed digital computer has made feasible the numerical solution of wave propagation problems in shells and the rapid development of electronic instrumentation, including laser holography,³ has made possible the experimental observation and measurement of wave propagation. These powerful numerical and experimental tools will, no doubt, see increasing future application. That there is great need for proven analytical methods for computing wave propagation phenomena is exemplified by the practice of requiring nearly all aerospace structures which are to be subjected to explosive environments to undergo a test of the full-scale structure and equipment using the actual explosive devices. Analytical methods have not yet been accepted in lieu of full-scale tests for predicting transient response due to explosive shock. It is, therefore, in the spirit of contributing to this important area of technology that the present paper is offered. No new theory is suggested. Rather, present analytical and computational methods are exploited and their potential revealed.

In order to compute the response of shells to wave generating forces, most workers in the field have concentrated their efforts on the method of finite differences or the method of characteristics. If modal methods are even mentioned, they are usually dismissed as being impractical due to slow convergence. This latter point was investigated in Ref. 4, and the conclusion was that modal methods are inadequate. However, most of these investigations use only the first few (5 or 6) modes. Recently developed computational methods^{5,6} have provided the capability efficiently to generate large numbers of modes (e.g., up to several hundred modes for each circumferential wave number) for orthotropic ring-stiffened shells of revolution, thus, opening up this class of structures to wave propagation studies by modal superposition.

The purpose of this paper is to demonstrate effective use of modal superposition solutions for studying wave propagation in finite-length shells of revolution. Solutions involving

Presented at the AIAA/ASME 11th Structures, Structural Dynamics and Materials Conference, Denver, Colo., April 22-24, 1970 (no paper number; published in bound volume of conference papers); submitted June 9, 1970; revision received February 1, 1971. The authors wish to express their appreciation to D. S. Catherines, B. J. Durling, and C. Pusey, who wrote the digital computer programs used to obtain the finite-element modal and finite-difference results presented in this paper.

* Head, NASTRAN Systems Management Office. Associate Fellow AIAA.

† Aerospace Engineer.

Table 1 Summary of analytical methods and shell theories

Numerical method	Initial velocity condition	Time varying edge condition	Shell theory
Modal superposition	✓	✓	Refs. 5 and 6
Finite differences	✓		Refs. 5 and 6
Method of characteristics		✓	Refs. 4, 7, and 8

only axisymmetric waves are presented, although the more general axisymmetric case does not pose any additional theoretical complications for the modal approach but does require additional computer time to obtain solutions. First, converged results for two different shells each with an initial-axial velocity distribution are presented. Here, modal superposition and finite-difference solutions are compared, and the results of convergence studies are discussed. Further evaluation of modal superposition solutions is presented for a time-varying axial displacement boundary condition for the same two shells, and comparison is made with the method of characteristics⁷ for both axial and radial displacements and axial stresses. Finally, axial and radial response attenuation by addition of a ring stiffener is demonstrated as an indication of a possible design technique for explosive shock. The notation is standard and is consistent with the references. The units employed are inch, pound, and seconds throughout.

Analysis

Two types of problems are studied in this paper: axisymmetric response of a cylindrical shell to an initial axisymmetric velocity at its center, and a time-varying edge condition. Three schemes for solution of the transient response or wave propagation problem are employed in combination with two different formulations^{4,5} of the shell equations (Table 1). Chou's formulation^{4,8} includes shear and rotatory inertia and, except for using the centroidal surface as the reference surface, is identical to that of Herrmann and Mirsky,⁹ who use the middle surface. The computer program of Ref. 7 mechanizes the solution of Chou's equations using the method of characteristics and it is this program, MCDIT 21, which was used to obtain the solutions by the method of characteristics presented later. The formulation and computer mechanization of Ref. 5 is used to obtain the modes used in obtaining the finite-element modal solutions, and equations of motion consistent with this formulation were solved using finite differences for comparisons. This formulation⁵ is that of Ref. 9 without the transverse shear and rotatory inertia effects.

Modal Approach

The essential ingredient for the effective use of modal superposition is the capability to generate, efficiently, a very large number of modes for a given shell. The basic procedure for obtaining the vibration modes which are used for the modal results presented in this paper is the finite-element method described in Refs. 5 and 6. The procedure for including ring stiffeners is described in Ref. 10. The strain-displacement relations used in Refs. 5 and 6 are those of Novozhilov,¹¹ and the strain energy is given by Ambartsumyan.¹² It is emphasized that the computational methods^{5,6} are capable of handling asymmetric response of a general shell of revolution, although the present study is restricted to the symmetric response of a cylindrical shell. Both initial velocity and time-varying coordinate conditions can be handled easily within the framework of the modal method. The approach is outlined as follows: the equations of motion produced by the

finite-element method are

$$[M]\{\ddot{y}\} + [K]\{y\} = \{f(t)\} \quad (1)$$

$$\text{with } \{y(0)\} = \{y\}_0 \text{ and } \{\dot{y}(0)\} = \{\dot{y}\}_0 \quad (2)$$

where $[M]$ and $[K]$ are mass and stiffness matrices for the free-free shell. To impose a zero motion condition on an edge coordinate or on any desired coordinate, say y_j , one must strike the j th rows and columns from $[M]$ and $[K]$ as discussed in Ref. 5.

For the initial velocity condition $\{f(t)\} = \{0\}$, $\{y\}_0 = \{0\}$ and $\{\dot{y}\}_0$ is specified over some portion of the shell. Imposing the fixed boundary conditions results in $[\bar{M}]\{\ddot{y}\} + [\bar{K}]\{y\} = \{0\}$ with $\{y(0)\} = \{0\}$ and $\{\dot{y}(0)\} = \{\dot{y}\}_0$ where the barred quantities indicate that the rows and columns corresponding to fixed coordinates have been deleted. For the time-varying edge condition

$$[M]\{\ddot{y}\} + [K]\{y\} = -\{m\}\ddot{y}_k - \{k\}y_k \quad (3)$$

$$\{y(0)\} = \{\dot{y}(0)\} = 0 \quad (4)$$

where $\{m\}$ and $\{k\}$ are the k th columns of $[\bar{M}]$ and $[\bar{K}]$, respectively, with the k th rows removed and the boldface quantities now indicate that, in addition to deletion of rows and columns corresponding to whatever fixed edge conditions are imposed, the k th row and column corresponding to the time-varying coordinate y_k also have been removed. (see, for example, pp. 300–308 of Ref. 13).

The modal matrix $[\phi]$ or $[\Phi]$ is comprised of solution vectors of either $[\bar{K} - \lambda\bar{M}]\{\bar{y}\} = 0$ (initial velocity condition) or $[K - \lambda M]\{y\} = 0$ (time-varying edge condition) and the modal equations are obtained using the familiar transformation

$$\{\bar{y}\} = [\bar{\phi}]\{\bar{q}\} \text{ or } \{y\} = [\phi]\{q\} \quad (5a)$$

For the time-varying edge condition the uncoupled modal equations take the form

$$\{\ddot{q}\} + [\lambda]\{q\} = [\phi]^T\{f(t)\} \quad (5b)$$

For all the cases considered in this paper the functions $f(t)$ were fifth-order polynomials in t , so that for a time-varying edge condition the i th equation of Eq. (5b) is of the form

$$\ddot{q}_i + \lambda_i q_i = a_0^{(i)} + a_1^{(i)}t + a_2^{(i)}t^2 + a_3^{(i)}t^3 + a_4^{(i)}t^4 + a_5^{(i)}t^5 \quad (5c)$$

$$q(0) = \dot{q}(0) = 0$$

Equations (5c) can be solved easily in closed form, thus, eliminating the need for a time-consuming numerical integration.

Finite Differences

A specialization of the energy expression in Ref. 5 to the response of a cylindrical shell and use of Lagrange's equations leads to a set of three partial differential equations which describe the transient response. For axisymmetric response, the equation for the circumferential response v is uncoupled from the other two equations and, hence, only the following two equations, with appropriate boundary conditions, must be solved to obtain the axial response u and the radial response w :

$$\partial^2 u / \partial t^2 = [Eh/\rho(1 - \nu^2)]\partial^2 u / \partial x^2 + [\nu Eh/\rho R(1 - \nu^2)]\partial w / \partial x \quad (6a)$$

$$\partial^2 w / \partial t^2 = -[Eh^3/12\rho(1 - \nu^2)]\partial^4 w / \partial x^4 - [Eh/\rho R^2(1 - \nu^2)]w - [\nu Eh/\rho R(1 - \nu^2)]\partial u / \partial x \quad (6b)$$

Use of central finite differences leads to the following system of coupled ordinary differential equations which were numeri-

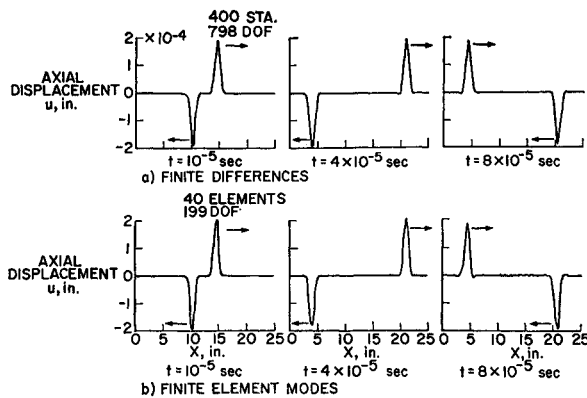


Fig. 1 Cylinder 1: converged axial displacement response to initial axial velocity.

cally integrated

$$d^2 u_n / dt^2 = [Eh / \rho(1 - \nu^2)] [(u_{n+1} - 2u_n + u_{n-1}) / \Delta x^2] + [vEh / \rho R(1 - \nu^2)] [(w_{n+1} - w_{n-1}) / 2\Delta x]$$

$$d^2 w_n / dt^2 = -[Eh^3 / 12\rho(1 - \nu^2)] [(w_{n+2} - 4w_{n+1} + 6w_n - 4w_{n-1} + w_{n-2}) / \Delta x^4] - [Eh / \rho R^2(1 - \nu^2)] w_n - [vEh / \rho R(1 - \nu^2)] [(u_{n+1} - u_{n-1}) / 2\Delta x]$$

and $w_{N+1} = w_{N-1}$, $w_{-1} = w_1$, $u_0 = u_N = w_0 = w_N = 0$, $w(x, 0) = \dot{w}(x, 0) = u(x, 0) = 0$, and $\ddot{u}(x, 0) = g(x)$ where $n = 1, 2, \dots, N - 1$.

Method of Characteristics

The MCDIT 21 computer code,⁷ which handles semi-infinite problems with zero initial conditions and time-varying boundary conditions, was used here. The reflected waves, presented later, for this code were provided by the authors of Ref. 7, who have recently modified that code to include finite-length cylinders. For the axisymmetric response of a cylindrical shell, the equations of motion in the notation of Ref. 7 are as follows:

$$u_{xx} - (1/c_p^2)u_{tt} = -(\nu/R)w_x$$

$$\psi_{xx} - (1/c_p^2)\psi_{tt} = (g/R\eta F_2)\psi + [(g + \eta\nu/R)/R\eta F_2]w_x \quad (7)$$

$$w_{xx} - (1/c_s^2)w_{tt} = (\nu/Rg)u_x - (1 + \eta\nu/gR)\psi_x + [(1 + \eta/R)/R^2g]w$$

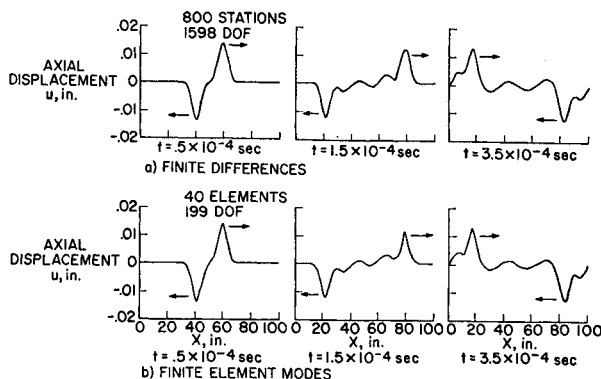


Fig. 2 Cylinder 2: converged axial displacement response to initial axial velocity.

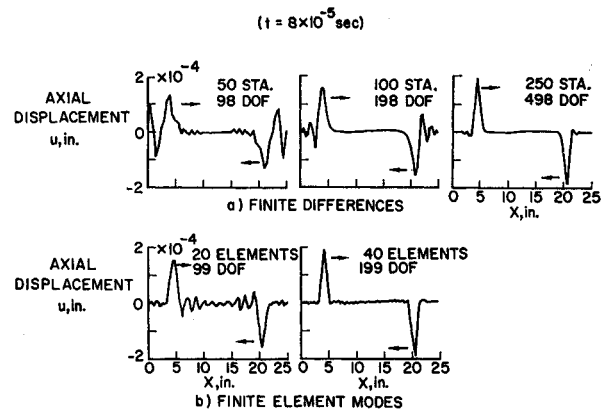


Fig. 3 Convergence studies for cylinder 1.

These equations are hyperbolic and therefore can be solved using the method of characteristics.

Results

In this section, comparisons of solutions by the modal method with solutions by finite differences and the method of characteristics are presented. The physical properties of the two cylinders studied are given in Table 2.

Modal vs Finite-Difference Solutions for Response to Initial Velocity Condition

The boundary conditions in the results presented in Figs. 1-4 are clamped-clamped. An initial velocity condition was imposed at the center of each shell as given in Table 3. The converged axial displacement response of cylinder 1 to the specified initial velocity is shown in Fig. 1. Although the results for the finite-difference method (Fig. 1a) employ nearly 800 degrees-of-freedom, the convergence studies which will be discussed subsequently indicate that 500 degrees-of-freedom are sufficient to produce a converged solution by this method. It can be seen that the solution obtained by the use of finite-element modes (Fig. 1b) depicts a traveling wave identical to that of the finite-difference solution, including the wave which is reflected from the boundary. Thus, it is evident that superposition of the finite-element modes yields a valid solution for this transient response or wave propagation problem.

The converged axial displacement response of cylinder 2 to the initial velocity (Table 3) is shown in Fig. 2. As will be shown in the discussion of convergence, for both of the methods, the number of degrees-of-freedom used to obtain

Table 2 Summary of cylinder properties

Cylinder 1		Cylinder 2		
	$L = 25"$ $R = 10"$ $h = .4"$ $E = 3 \times 10^7$		$L = 100"$ $R = 5"$ $h = .05"$ $E = 10^7$ psi	
	$\gamma = .283$ lb/in. ³ $\nu = .3$ $C_p = 213,160$ ips $C_s = 116,730$ ips $k^2 = 0.87$		$\gamma = .116$ lb/in. ³ $\nu = .3$ $C_p = 191,200$ ips $C_s = 105,521$ ips $k^2 = 0.87$	
			$E = 10^7$ $\gamma = .116$ lb/in. ³ $\nu = .3$	

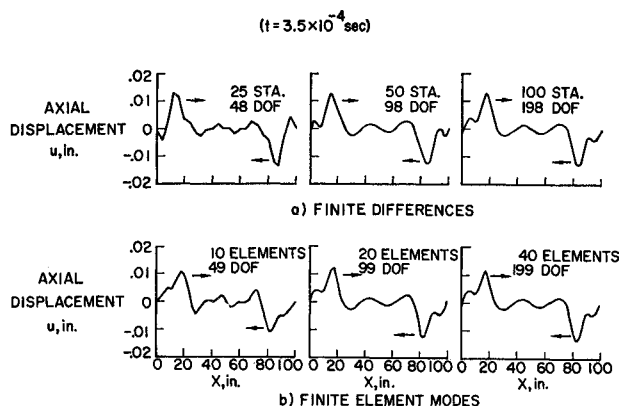


Fig. 4 Convergence studies for cylinder 2.

the results for Fig. 2 is greater than the number actually required to demonstrate that the results are in fact converged. As in the case of cylinder 1, both the finite-difference and modal solutions of Eqs. (6) give identical results.

The results of the convergence studies for cylinder 1 are shown in Fig. 3. The studies are based on the reflected wave at $t = 8 \times 10^{-5}$ sec. Comparison of parts a and b indicates that 498 degrees-of-freedom by the finite-difference method and 199 degrees-of-freedom by the modal method yield results which are practically identical to the finite-difference results with 798 degrees-of-freedom shown in Fig. 1a. Figure 3 also illustrates that 199 finite-element modes yield a converged solution for this case, while substantially more degrees-of-freedom are required by the finite-difference method. In this connection, note that 498 finite-difference degrees-of-freedom (250 stations) are required to give a solution which compares favorably with the solution obtained by 40 finite elements (199 degrees-of-freedom).

The convergence studies for cylinder 2 are shown in Fig. 4. The results are based upon the reflected wave at $t = 3.5 \times 10^{-4}$ sec. Figure 4 shows that 99 degrees-of-freedom by the modal method and 198 degrees-of-freedom by the finite-difference method give results which are practically identical to the finite-difference results with 1598 degrees-of-freedom shown in Fig. 2a.

Numerical dispersion study

In order to study the dispersive effect of the numerical methods, the one-dimensional wave equation for a string with an initial displacement condition was solved by two different techniques, and the solutions were compared with D'Alembert's solution. The solution obtained using 50 exact modes was coincident with D'Alembert's solution. The solution was also obtained by the finite-element modes. Study of the solution obtained by finite-element modes indicates that once the method is converged to the initial condition with accurate modes, the resulting solution for the propagating wave is acceptable, and the dispersion introduced is negligible. The modal method introduced unacceptable dispersion only when the number of accurate modes was insufficient to obtain convergence to the initial condition.

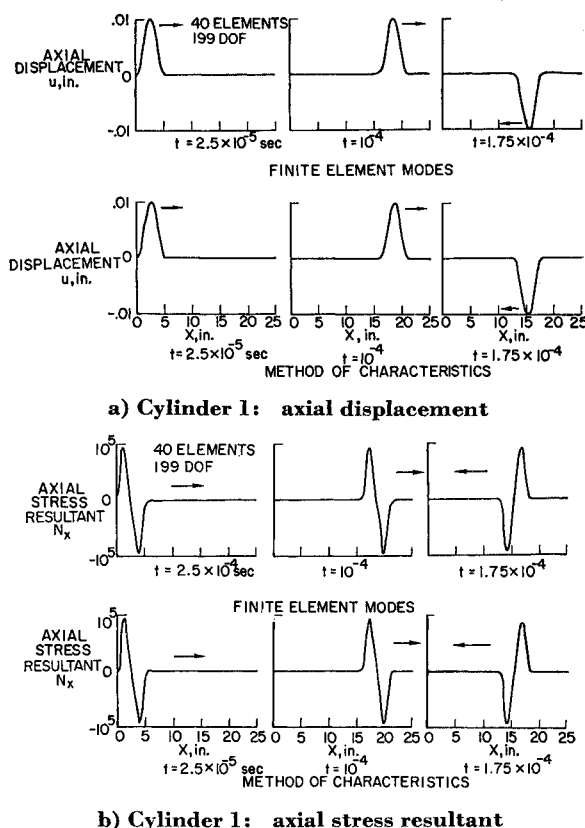


Fig. 5 Response to time-varying boundary condition.

Selection of accurate modes

For initial condition problems, the results of the numerical dispersion study suggest that convergence to the initial conditions with accurate modes is sufficient to guarantee a satisfactory solution for all later times. In this connection, convergence studies using the finite-element modes can be deceiving. If the solution to the transient problem is found to depend heavily upon some of the higher frequency modes, the tendency is to reject the solution on the assumption that higher frequency modes are likely to be inaccurate. This assumption is not necessarily valid. For example, the 20-finite-element solution for cylinder 2 depends strongly upon the 66th mode out of a total number of 99 modes for that case. Nevertheless, comparison of Figs. 2a for $t = 3.5 \times 10^{-4}$ sec and Fig. 4b clearly indicates that the 20-finite-element solution is converged. The 66th mode for this case is a high-frequency mode with a simple shape. Studies of a freely supported cylinder (for which an exact solution is available) have verified that the modal procedure can produce accurate high-frequency modes. For example, in the freely supported case, the 70th mode out of 103 agreed very well with a true mode of the system—a simply-shaped, high-frequency mode. Thus higher frequency modes obtained by the modal procedure should not automatically be rejected as inaccurate. More investigation is required to determine a satisfactory method of identifying the accurate modes.

Table 3 Summary of equations for initial velocity conditions

Cylinder	Initial condition
1	$\dot{u}(x,0) = \begin{cases} 0 & 0 \leq x \leq 11.25 \\ -512(x - 11.25)^2 + 409.6(x - 11.25)^3 & 11.25 \leq x \leq 12.5 \\ 512(13.75 - x)^2 - 409.6(13.75 - x)^3 & 12.5 \leq x \leq 13.75 \\ 0 & 13.75 \leq x \leq 25 \end{cases}$
2	$\dot{u}(x,0) = \begin{cases} 0 & 0 \leq x \leq 40 \\ -64(x - 40)^2 + 6.4(x - 40)^3 & 40 \leq x \leq 50 \\ 64(60 - x)^2 - 6.4(60 - x)^3 & 50 \leq x \leq 60 \\ 0 & 60 \leq x \leq 100 \end{cases}$

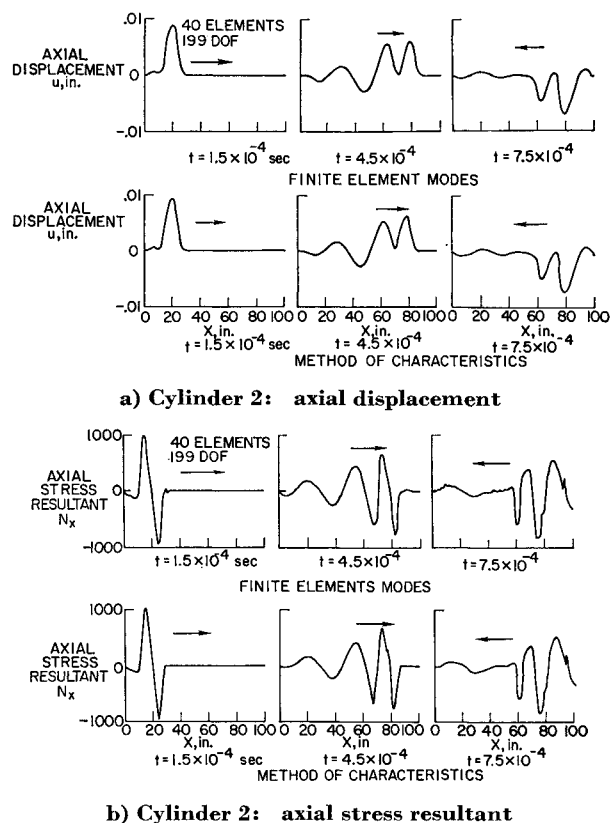


Fig. 6 Response to time-varying boundary condition.

Modal vs Method of Characteristics Solution for Response to Time-Varying Edge Condition

The boundary conditions in the converged results presented in Figs. 5-7 are clamped-clamped as for the previous results except that a bell-shaped, time-varying motion input $u(0,t)$ was applied to the end of the cylinder with $u(0,t) = 0$ upon completion of the motion. The time-varying input is described in Table 4.

Figure 5a shows the axial displacement response of cylinder 1 to the specified time-varying edge condition as obtained by both the finite-element method and the method of characteristics. The axial stress resultants computed using $N_x = [Eh/(1 - \nu^2)][\partial u/\partial x + (\nu/R)w]$ for corresponding times are presented in Fig. 5b. As can be seen in Fig. 5, both the displacements and axial stress resultants obtained by the modal superposition method are coincident with those obtained by the method of characteristics.

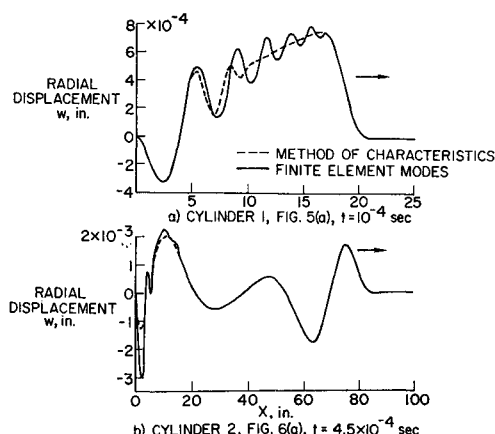


Fig. 7 Coupled radial response for axial displacement, time-varying boundary condition.

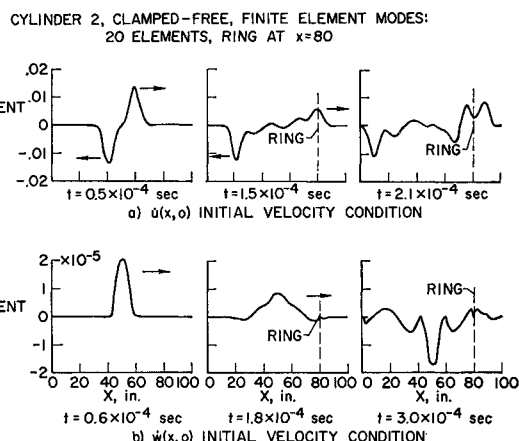


Fig. 8 Attenuation effect of ring.

The corresponding results for cylinder 2 are shown in Fig. 6. For this cylinder, the response is highly dispersive following the passage of the wave front as indicated by both analytical methods. As was the case for cylinder 1, the axial displacements and stress resultants obtained by the finite-element method are practically identical to the solutions obtained by the method of characteristics.

Figure 7 shows the associated response in the radial direction for both cylinders. For the radial response, the solutions given by the two methods are in generally good agreement, although there are some discrepancies behind the wave front. The position and shape of the leading edge of the wave is the same for both methods.

Attenuation Effect of a Ring on Response to Initial Axial and Radial Impulses

In order to demonstrate the modal method further, the responses to an initial axial and an initial radial velocity were separately computed for a clamped-free cylinder with a ring stiffener at $x = 80$ in. from the clamped end. Cylinder 2 was selected and axisymmetric modes were computed for clamped-free boundary conditions using a 20 equally spaced finite-element analysis. The dynamic effects of an aluminum, rectangular section ring with thickness in the axial direction of 0.4 in. and depth in the radial direction of 1.2 in. were included using the approach of Ref. 10. The initial axial velocity condition is given by the second equation of Table 3. The initial radial velocity condition is described as follows:

$$\begin{aligned}
 & 0 \quad 0 \leq x \leq 40 \\
 & [(x - 40)/20]^3 [80 - 12(x - 40) + 0.48(x - 40)^2] \quad 40 \leq x \leq 50 \\
 & [(60 - x)/20]^3 [80 - 12(60 - x) + 0.48(60 - x)^2] \quad 50 \leq x \leq 60 \\
 & 0 \quad 60 \leq x \leq 100
 \end{aligned} \quad (8)$$

The choice of cylinder 2 for this computation was based on its relatively low thickness to radius ratio of 0.01 for which it was felt that the transverse shear and rotatory inertia effects

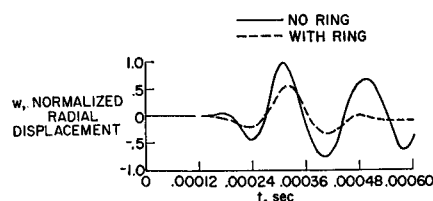
Fig. 9 Time history response for $\dot{w}(x,0)$ initial velocity condition at $x = 85$.

Table 4 Summary of equations for time-varying edge conditions

Cylinder		Time-varying edge condition	
1	$u(0,t) =$	$\begin{cases} 5.12 \times 10^{12}t^3 - 6.144 \times 10^{12}t^4 \\ \quad + 1.966 \times 10^{22}t^5 \\ 0.32 - 9.6 \times 10^4t + 1.152 \times 10^{10}t^2 \\ \quad - 6.656 \times 10^{14}t^3 \\ \quad + 1.8432 \times 10^{19}t^4 \\ \quad - 1.966 \times 10^{23}t^5 \\ 0 \end{cases}$	$\begin{cases} 0 \leq t \leq 1.25 \times 10^{-5} \\ 1.25 \times 10^{-5} \leq t \leq 2.5 \times 10^{-5} \\ 2.5 \times 10^{-5} \leq t \end{cases}$
		$\begin{cases} 8 \times 10^{11}t^3 - 2.4 \times 10^{16}t^4 \\ \quad + 1.92 \times 10^{20}t^5 \\ 0.32 - 2.4 \times 10^4t + 7.2 \times 10^7t^2 \\ \quad - 1.04 \times 10^{13}t^3 \\ \quad + 7.2 \times 10^{16}t^4 \\ \quad - 1.92 \times 10^{20}t^5 \\ 0 \end{cases}$	$\begin{cases} 0 \leq t \leq 5 \times 10^{-5} \\ 5 \times 10^{-5} \leq t \leq 10^{-4} \\ 10^{-4} \leq t \end{cases}$
2	$u(0,t) =$		

would be negligible. In this regard, it is well to recall that the theory employed in Refs. 5 and 6 is that of Novozhilov [see, for example, Eqs. (6)] which neglects the effects of transverse shear and rotatory inertia.

The axial and radial responses for several times are shown in Fig. 8, in which it can be observed that the disturbance propagates at the plate velocity of 191,200 in./sec. Time histories of the radial response at $x = 85$ in. shown in Fig. 9 indicate that significant benefit is derived from the ring upstream at $x = 80$.

Discussion

The results presented in this paper have employed three methods of solution and two sets of shell equations. Equations (6) based on Novozhilov's formulation can be obtained from Eqs. (7) by transforming from the centroidal to the middle surface and neglecting transverse shear and rotatory inertia. This procedure reduces Eqs. (7) from a totally hyperbolic system which can be solved using the method of characteristics to Eqs. (6) which cannot be thus solved. Only the equation in axial displacement u is unaffected. Equations (6) should not be used when the combination of input and shell characteristics is such that the effects of transverse shear and rotatory inertia are in doubt. The method of characteristics is uniquely associated with a hyperbolic system of equations. However, the modal superposition method can be employed with any formulation of the equations of motion.

Initial Velocity Condition

The results of Figs. 1-4 indicate that both the finite-difference and modal solutions converge to the solution of Eqs. (6) for both cylinders for the initial conditions of Table 3. The axial displacement waves travel at the respective plate velocities of each of the two cylinders. However, the results of Figs. 3 and 4 indicate that the modal method requires fewer degrees-of-freedom to produce a converged solution. Also in the modal approach, the participation of each mode is known. Therefore, by using suitable criteria for determining the quality of a given mode, the over-all quality of the transient response solution can be evaluated. At present, an easily applied, quantitative criterion has not been established. Nonetheless, the modal approach is felt to offer much important insight into transient response problems including wave propagation.

Time-Varying Edge Condition

The results of Figs. 5 and 6 which involve finite-element modal solutions of Eqs. (6) and method of characteristics solutions of Eqs. (7) for the time-dependent boundary conditions of Table 4 indicate that both solutions produce coincident results for axial displacement and stress waves. The modal approach does, however, allow efficient computation of long-time response including reflected waves. In this case,

as for the initial velocity condition of Figs. 1-4, the u and w motions of cylinder 2 are more highly coupled than cylinder 1 resulting in the appearance of dispersion effects for cylinder 2 due to loss of energy to radial motion.

The results shown in Fig. 7 continue the comparisons of Figs. 5 and 6 to the radial response of both cylinders. The differences are due to the differences between Eqs. (6) and (7) and not to the method of solution. Coupling between u and w in both equations is through first partial derivatives. The radial response computed by both methods for both cylinders is in substantially good agreement indicating that neglecting transverse shear and rotatory inertia [Eqs. (6)] has not adversely influenced the coupled radial response, w , when the input is on the axial displacement, u .

Ring Attenuation Study

Because most practical applications involve an input in either the axial or radial direction, the initial axial velocity condition given by the second equation of Table 3 and the radial velocity condition of Eq. (8) were separately imposed on cylinder 2 clamped-free to indicate the ease with which the modal method can be employed to investigate the effects of proposed shock-attenuation schemes. As shown in Fig. 8, both the axial and radial disturbances propagate at the plate velocity c_p for the shell; however, the radial motion of Fig. 8b appears to be more of a vibration response (i.e., a standing wave) than a traveling displacement wave. In both cases, the ring provides significant attenuation. The time histories given in Fig. 9 show that the ring attenuates the radial response at a point downstream by about 50% over the response when no ring is present.

The radial response results shown in Fig. 8b appeared to be converged solutions, but because there was no available alternate solution to the radial response case under discussion and because it was felt that transverse shear and rotatory inertia might be significant for this case, a check uniquely available to the modal approach was invoked. The individual modes contributing to the response were examined. Specifically, the modes required to converge to the response at $t = 0.6 \times 10^{-4}$ sec were first determined. For convergence, the first 76 of a total of 102 modes were required. Second, the modes were examined from two points of view 1) comparison to exact solution of the axisymmetric modes for Eqs. (6); 2) qualitative evaluation of the importance of transverse shear and rotatory inertia effects.

It was determined that 1) a solution using modes from greater than a 20-finite-element formulation would be desirable in order to be certain that the contributing modes were exact solutions to Eqs. (6) and that 2) the effects of transverse shear and rotatory inertia could possibly be of marginal importance.

The authors followed through on these two items as follows: First, the convergence of the radial response results shown in

Fig. 8b was confirmed by computing a 40-finite-element modal solution which produced results coincident with those of Fig. 8b. Second, the energy expressions in the finite-element formulation were modified to include the effects of transverse shear and rotatory inertia for the special case of a right circular cylinder. The results, thus obtained, using a 20-finite-element modal solution were coincident with those previously obtained using the Novozhilov theory of Ref. 5. Thus, transverse shear and rotatory inertia effects were determined to be inconsequential for this case.

Conclusions

The modal superposition method of this paper which rests on an efficient generator of a sufficient number of modes for a selected shell and closed-form solution of the modal equations is an effective method for the analysis of wave propagation in shells and, for the class of problems studied, offers some distinct advantages for computing the transient response of shells including wave propagation: 1) Once a set of modes has been generated, the response at any desired time and for a wide variety of initial conditions or forcing functions given as polynomials can be computed with negligible additional computer time, whereas with either finite differences or the method of characteristics, the complete problem must be reinitiated. 2) The exact participation of each mode at each instant of time is available, so that the contribution from questionable modes is easily determined. The modal approach, therefore, provides greater insight into the transient analysis of shells than either finite differences or the method of characteristics. 3) The modal method is the most efficient for the problems studied and produces converged solutions requiring fewer degrees-of-freedom than the finite-difference method. 4) Based on the availability of the mode generating algorithms of Ref. 5 for general shells of revolution including the effects of ring stiffeners, the capability presently exists for analysis of the effects of, and design for, explosive shock or other wave generating phenomena.

References

- ¹ Kolsky, H., *Stress Waves in Solids*, Dover, New York, 1963.
- ² Miklowitz, J., ed., *Wave Propagation in Solids*, ASME, 1969.
- ³ Aprahamian, R. and Evensen, D. A., "Applications of Holography to High-Frequency Vibrations and Transient Response," Presented at 40th Shock and Vibration Symposium, The Shock and Vibration Information Center, Naval Research Lab., Hampton, Va., Oct. 21-23, 1969.
- ⁴ Chou, P. C., "Analysis of Transient Structural Response by the Method of Characteristics," CR-66691, 1968, NASA.
- ⁵ Adelman, H. M., Catherines, D. S., and Walton, W. C., Jr., "A Method for Computation of Vibration Modes and Frequencies of Orthotropic Thin Shells of Revolution Having General Meridional Curvature," TN D-4972, 1969, NASA.
- ⁶ Adelman, H. M. and Catherines, D. S., "A Geometrically Exact Finite Element for Thin Shells of Revolution," AIAA Paper 69-56, New York, 1969.
- ⁷ Mortimer, R. W. and Hoburg, J. F., "MCDIT 21—A Computer Code for One-Dimensional Elastic Wave Problems," CR-1306, 1969, NASA.
- ⁸ Chou, P. C., "Analysis of Axisymmetric Motions of Cylindrical Shells by the Method of Characteristics," *AIAA Journal*, Aug. 1968, Vol. 6, No. 8, pp. 1492-1497.
- ⁹ Herrmann, G. and Mirsky, I., "Nonaxially Symmetric Motions of Cylindrical Shells," *The Journal of the Acoustical Society of America*, Vol. 29, No. 10, Oct. 1957, pp. 1116-1123.
- ¹⁰ Steeves, E. C., Durling, B. J., and Walton, W. C., Jr., "A Method for Computing the Response of a General Axisymmetric Shell With an Attached Asymmetric Structure," *AIAA Structural Dynamics and Aeroelasticity Specialist Conference*, AIAA, New York, 1969.
- ¹¹ Novozhilov, V. V., *Thin Shell Theory*, 2nd ed., translated by P. G. Lowe, Noordhoff Ltd., Groningen, Holland, c. 1964, pp. 23-24.
- ¹² Ambartsumyan, S. A., "Theory of Anisotropic Shells," TT F-118, 1964, NASA.
- ¹³ Meirovitch, L., *Analytical Methods in Vibrations*, Macmillan, New York, 1967.